



1 Quantifying the contribution of anthropogenic influence to the
2 East Asian winter monsoon in 1960–2012

3
4 Xin Hao*^{1,2}, Shengping He^{4,1}, Huijun Wang^{1,2,3}, Tingting Han^{1,2}

5 ¹ Collaborative Innovation Center on Forecast and Evaluation of Meteorological
6 Disasters/Key Laboratory of Meteorological Disaster, Ministry of Education, Nanjing
7 University for Information Science and Technology, Nanjing 210044, China

8 ² Nansen-Zhu International Research Centre, Institute of Atmospheric Physics, Chinese
9 Academy of Sciences, Beijing 100029, China

10 ³ Climate Change Research Center, Chinese Academy of Sciences, Beijing 100029, China

11 ⁴ Geophysical Institute, University of Bergen and Bjerknes Centre for Climate Research,
12 Bergen 0025, Norway

13
14 Corresponding author: Xin Hao, haoxlike91@163.com

15
16 Abstract

17 The East Asian winter monsoon (EAWM) can be greatly influenced by many factors that can
18 be classified as anthropogenic forcing and natural forcing. Here we explore the contribution of
19 anthropogenic influence to the change in the EAWM over the past decades. Under all forcings
20 observed during 1960–2013 (All-Hist run), the atmospheric general circulation model is able to
21 reproduce the climatology and variability of the EAWM-related surface air temperature and 500
22 hPa geopotential height, and shows a statistically significant decreasing EAWM intensity with a
23 trend coefficient of $\sim -0.04 \text{ yr}^{-1}$ which is close to the observed trend. By contrast, the simulation,
24 which is driven by the same forcing as All-Hist run but with the anthropogenic contribution to
25 them removed, shows no decreasing trend in the EAWM intensity. By comparing the simulations
26 under two different forcing scenarios, we further reveal that the responses of the EAWM to the
27 anthropogenic forcing include a rise of 0.6°C in surface air temperature over the East Asia as well
28 as weakening of the East Asia trough, which may result from the poleward expansion and
29 intensification of the East Asian jet forced by the change of temperature gradient in the



30 troposphere. Additionally, compared with the simulation without anthropogenic forcing, the
31 frequency of strong (weak) EAWM occurrence is reduced (increased) by 45% (from 0 to 10/7).
32 These results indicate that the weakening of the EAWM during 1960–2013 may be mainly
33 attributed to the anthropogenic influence.

34 **Key words:** anthropogenic influence, East Asian winter monsoon, contribution

35 1. Introduction

36 The East Asian winter monsoon (EAWM) is one of the most dominant climate
37 systems in East Asia. It greatly affects the disastrous winter weather such as cold
38 waves, snowstorms, air pollutions, and spring duststorms (Li et al., 2016; Li and
39 Wang, 2013; Wang et al., 2009; Zhou et al., 2009; Chang et al., 2006). Prominent
40 circulation components from surface to the upper troposphere associated with
41 temperature condition during the boreal winter are dynamically linked to the EAWM.
42 At surface, the EAWM contains the cold Siberian high dominated over the East Asian
43 continent and the warm Aleutian low located in the high-latitude North Pacific, which
44 accompanies with prevailing northwesterly winds in the low-level troposphere (He
45 and Wang, 2013; Wang and Jiang, 2004; Gong et al., 2001; Guo 1994; Lau and Li,
46 1984). At 500 hPa locates the East Asian trough which determines the outbreak and
47 intensity of the EAWM (He et al., 2013; Cui and Sun, 1999; Sun and Li, 1997). In the
48 upper troposphere, a key component of the EAWM is the East Asian jet with its
49 maximum core being located to the southeast of Japan (Jhun and Lee, 2004; Boyle
50 and Chen, 1987). Concurrent with the change of these atmospheric circulation, the
51 change of winter surface air temperature (SAT) over East Asia is closely related to the
52 variation in the EAWM (Hao and He, 2017; Lee et al., 2013; Wang et al., 2010).

53 Above primary components of the EAWM system are subject to obvious changes
54 under the influence of global warming (e.g., Li et al., 2018; Li et al., 2015; IPCC,
55 2013; Hori and Ueda, 2006; Kimoto, 2005; Zhang et al., 1997). Under different global
56 warming scenarios, thermodynamic contrast between the East Asian continent and the
57 Pacific Ocean is reduced uniformly characterized with weakening of the East Asian
58 trough (EAT) as well as the East Asian jet, indicating a weakening of the EAWM (e.g.,



59 Xu et al., 2016; Kimoto, 2005). Previous studies based on Coupled models generally
60 agree on the effect of global warming on the EAWM (Hong et al., 2017; Xu et al.,
61 2016; Kimoto, 2005; Hu et al., 2000). However, previous studies mainly conduct
62 qualitative research on the potential influence of the global warming, it's still unclear
63 to what extent can the anthropogenic activities impact the EAWM. This study aims to
64 quantitatively estimate the contribution of increasing anthropogenic emissions over
65 the past decades to the change of the EAWM, which is essential for the projection of
66 the EAWM in the future.

67

68 2. Data and Method

69 Monthly mean dataset including SAT, 500 hPa geopotential height and 250 hPa
70 zonal wind is obtained from National Center for Environmental Prediction/National
71 Center for Atmospheric Research (NCEP/NCAR) Reanalysis 1 dataset at a horizontal
72 resolution of $2.5^\circ \times 2.5^\circ$ (Kalnay et al., 1996). Hereafter it is referred to as
73 "observations". To explore the contribution of the anthropogenic emissions to climate
74 change, two different simulations from the C20C+ Detection and Attribution Project
75 (<http://portal.nersc.gov/c20c/data.html>) are compared in the context of two different
76 forcing scenarios. One is the *All-Hist* which was forced with time-vary boundary
77 conditions (e.g., greenhouse gas concentrations, anthropogenic and natural aerosols,
78 ozone, solar luminosity, land cover, sea surface temperatures and sea ice) observed
79 during the past few decades. The other is the *Nat-Hist* which was forced with
80 observed sea surface temperature and sea ice concentrations from which the
81 anthropogenic contribution has been removed (please refer to
82 <http://portal.nersc.gov/c20c/data.html> for more details). Meanwhile, the natural
83 external forcing such as greenhouse gas concentrations and aerosols was set to
84 preindustrial levels. We analyse the simulations by an atmospheric general
85 circulation model HadGEM3-A-N216 (Christidis et al., 2013; approximately $0.56^\circ \times$
86 0.83° horizontally) available from the C20C+ Detection and Attribution, which has
87 been used to conduct the above two sets of experiments from 1960 to 2013. Both



88 All-Hist and Nat-Hist runs include 15 ensemble members. Each realization in the two
89 scenarios differs from the other only in its initial state. The ensemble-mean of the runs
90 number 1, 2, 5, 13, 14, and 15 (which show a better performance in simulating
91 interannual, decadal and linear trend change of EAWM) under the All-Hist scenarios
92 agrees best with the reanalysis dataset (such as climatology, interannual and decadal
93 change of EAWM; evaluation of other runs of model shown in supplementary).
94 Therefore, the simulations of these 6-members ensemble are used in this study.

95 In this study, we focus on the winter mean which is the average of December,
96 January and February (e.g., the winter 2008 refers to the boreal winter of 2008/2009).
97 Two intensity indices are used to describe the variability of the EAWM: one is defined
98 as the area-averaged height geopotential at 500 hPa in 35° – 45° N, 125° – 145° E
99 (EAWMI_HGT; Sun and Li, 1997); the other is defined as the area-averaged SAT in
100 25° – 45° N, 105° – 145° E (EAWMI_SAT; Lee et al., 2013). Both area-averaged values
101 are multiplied by -1 so that positive values correspond to strong EAWM; 9-year
102 running mean of the index represents the interdecadal variability of the EAWM.

103

104 3. Results and Discussions

105 3.1 Assessment of the atmospheric circulation pattern simulated by model in All-Hist 106 runs

107 The EAWM is characterized by northerly winds over East Asia, the Siberian high,
108 the Aleutian low, the deep East Asian trough, the upper tropospheric East Asian jet
109 stream, as well as the cold and dry conditions over East Asia (e.g., Hao et al., 2016;
110 Lee et al., 2013; He and Wang, 2013; Wang and Jiang, 2004; Sun and Li, 1997). In
111 this study, the performance of the HadGEM3-A-N216 model in simulating the above
112 characteristics of the EAWM is firstly evaluated by comparing the corresponding
113 results in the All-Hist runs with reanalysis dataset in the period of 1960–2012.

114 Figures 1a-d show the climatology of the SAT and 500 hPa geopotential height
115 in winter from the observations and simulations in the All-Hist run. The winter SAT
116 climatology over East Asia in simulations (Fig. 1a) is generally consistent with the



117 observed counterpart (Fig. 1b). The model has successfully reproduced the dominant
118 features of East Asian winter SAT such as the northwest-to-southeast temperature
119 gradient, the 0°C isotherm of SAT stretching from western China (around 27.5°N)
120 northeastward to north Japan (around 42.5°N), the cold center located over the
121 Tibetan Plateau (Figs. 1a and 1b). Compared with the observations, the simulated SAT
122 shows apparent cold bias over the north of 40°N but less bias over the south of 40°N.
123 In the middle troposphere, the main features (position of axis and intensity) of the
124 EAT are also generally reproduced by the model. The simulated SAT in 25°–45°N,
125 105°–145°E (Lee et al., 2013) and 500 hPa geopotential height in 35°–45°N, 125°–
126 145°E (Sun and Li, 1997) used for the EAWM indices show high spatial correlations
127 with the observations (Fig. 1e), which are exceed 0.99. Additionally, high spatial
128 correlations of the simulated SAT and 500 hPa geopotential height with the
129 observation are accompanied by small root mean square errors (Fig. 1e). It means that
130 the All-Hist runs have well simulated the EAWM climatology.

131 The variability of the EAWM is also compared between the simulations and the
132 observations. It is found that the correlations between the simulated EAWM indices
133 and the observed EAWM indices are 0.3 for EAWMI_SAT and 0.31 for
134 EAWMI_HGT, respectively (Fig. 2), which are statistically significant. Additionally,
135 the interdecadal variability of the EAWM indices are closely correlated between the
136 simulations and the observation with correlation coefficients of 0.7 for EAWMI_SAT
137 and 0.76 for EAWMI_HGT (Fig. 2). The result suggests that the All-Hist runs have
138 well simulated the interannual and interdecadal variability of the EAWM and can be
139 further used to investigate the anthropogenic impact on the EAWM.

140

141 3.2 Contribution of anthropogenic influence to the East Asian winter monsoon

142 To investigate the anthropogenic contribution to the change of the EAWM, we
143 compare the EAWM in the All-Hist runs with those in the Nat-Hist runs. Both of the
144 EAWM indices in the All-Hist runs show statistically significant decreases over the
145 past decades, with trend coefficients of -0.044 (yr^{-1}) and -0.038 (yr^{-1}), respectively,
146 which are similar to the observed trends (-0.023 and -0.02 , respectively; Fig. 2). By



147 contrast, the EAWM indices in Nat-Hist run show an increasing trend, instead (Fig. 2).
148 It suggests that the increasing anthropogenic emissions in the past decades may
149 contribute to the weakening of the EAWM.

150 Figure 3 displays the composited differences of the simulated winter SAT and
151 500 hPa geopotential height between the All-Hist runs and in the Nat-Hist runs, which
152 approximately reflect the response of the EAWM to anthropogenic forcing. The
153 composited differences show clearly that winters with anthropogenic forcing see
154 apparent warmer anomalies over most parts of East Asia except for southeast China as
155 well as warmer conditions over the western North Pacific (Fig. 3a). Such a response is
156 similar to the one revealed by previous CMIP5 studies (Hong et al., 2017; Xu et al.
157 2016). Xu et al. (2016) suggested that the large positive anomalies over high-latitude
158 western North Pacific are due to a north ward shift of the significantly intensified
159 Aleutian low induced by the melting sea ice in the Bering Sea and Okhotsk Sea (Gan
160 et al., 2017). Quantitatively, compared with the situation without anthropogenic
161 influence, the wintertime SAT averaged over (20 °–60 °N, 100 °–140 °E) increases by
162 0.6°C over the last half-century due to anthropogenic influence (Fig. 3a). At middle
163 troposphere, responses of the 500 hPa geopotential height to anthropogenic forcing
164 shows obviously positive anomalies over East Asia with a value of 15.7 m, implying a
165 shallower EAT which results in less powerful cold air to East Asia (Fig. 3b). The
166 model simulations indicate clearly that the anthropogenic influence may induce a
167 weaker EAWM.

168 It should be noted that, in the low-level troposphere, the high-latitude warming
169 induced by the anthropogenic forcing is apparently stronger than the warming at
170 lower-latitudes (Fig. 4a), which is the so-called “polar amplification” (Meehl et al.,
171 2007; Collins et al., 2013). Meanwhile, in the high-level troposphere, obviously
172 warming occurs over the tropical regions and the Arctic, but cooling occurs over the
173 high-latitude regions under the anthropogenic influence (Fig. 4a). As a result, a
174 broadening and intensifying Hadley circulation appears, which is consistent with the
175 observed phenomena revealed by previous studies that a poleward expansion and
176 intensification of the winter Hadley circulation in the past few decades (Hu and Fu,



177 2007; Mitas and Clement, 2005; Hu et al., 2005). Such a change in the Hadley
178 circulation implies a poleward shift of the East Asian jet (Fig. 4b), together with a
179 reinforcement and expansion of Western Pacific subtropical high and an increase of
180 SLP in the high-latitude East Asia (Fig. 4c). The change of SLP also indicates a weak
181 decrease of the Siberian high and an intensified Aleutian low. Thus, under the
182 anthropogenic influence, significant easterly anomalies occur in the mid- and
183 high-latitude of East Asia and significant southerly anomalies occur in the
184 low-latitude of East Asia (Fig. 4c), leading to a subdued EAWM. We further explore
185 the contribution of anthropogenic influence to the occurrence of strong/weak EAWM.
186 The case with the normalized index larger than 1.0 (smaller than -1.0) is defined as a
187 strong (weak) EAWM event. The number of the strong/weak EAWM events is shown
188 in Fig. 5. The two observed EAWM indices display 10 (8) and 9 (9) strong (weak)
189 EAWM events during 1960–2012, respectively. Interestingly, the two simulated
190 EAWM indices in the All-Hist run display 11 (10) and 11 (7) strong (weak) EAWM
191 events, respectively. The number of strong or weak EAWM events forced by the
192 observed time-varying boundary conditions during the past few decades (All-Hist run)
193 is very close to the number in observations. However, during 1960–2012, the
194 simulated two EAWM indices in the Nat-Hist runs display 21 (0) and 19 (0) strong
195 (weak) EAWM events, which is remarkably different from the number in the All-Hist
196 runs as well as the observations. It implies that, in the past decades, the frequency of
197 occurrence of strong EAWM may have reduced by 45% due to the anthropogenic
198 forcing and the anthropogenic forcing is a dominant contributor to the occurrence of
199 weak EAWM.

200

201 4 Conclusion

202 The contribution of the anthropogenic influence to the climatology, trends, and
203 the frequency of occurrence of strong/weak EAWM is explored in this study based on
204 numerical simulations. Firstly, we evaluate the performance of the climate model
205 (HadGEM3-A-N216) in simulating the climatology of wintertime circulation over



206 East Asia and variation of EAWM indices during 1960–2012. The winter-mean states
207 of SAT and 500 hPa geopotential height related to the EAWM in the All-Hist runs
208 resemble well those in observation with spatial correlation coefficients of greater than
209 0.99. Also, the interannual and interdecadal variation of the EAWMI_HGT and
210 EAWMI_SAT can be well reproduced by the model under All-Hist scenario. Because
211 of the well performance of the All-His runs in simulating the EAWM indices and
212 winter-mean atmospheric circulation over the East Asia, the exploration about
213 changes of the EAWM induced by anthropogenic influence is considered reliable.

214 Under All-Hist scenario, the EAWM indices have significantly decline trends
215 over the past decades, which are consistent with those in observations, indicating that
216 the weakening of the EAWM could be simulated by the climate model with all forcing.
217 However, the EAWM indices do not have such trends in the Nat-Hist runs. Compared
218 the area-averaged SAT and 500 hPa geopotential height related to the EAWM for the
219 period of 1960–2012 between two families of experiments, it is found that
220 anthropogenic emissions induce obviously positive SAT anomalies in the most region
221 of East Asia and a weakened EAT, as shown in previous results (Hu et al., 2000; Hori
222 and Ueda, 2006; Xu et al. 2016; Hong et al., 2017; Hong et al., 2017). Additionally,
223 11 (11) strong EAWM events and 10 (7) weak EAWM events are forced by All-Hist
224 scenario during 1960–2012, which are close to the frequency of occurrence of strong
225 and weak EAWM in observations, while 21 (19) strong EAWM events and 0 (0) weak
226 EAWM event are forced by Nat-Hist scenario. Overall, under anthropogenic influence,
227 during 1960–2012, the EAWM continued to be weakened, and the frequency of
228 occurrence of strong (weak) EAWM had decreased (increased) by 45% (from 0 to
229 10/7). The poleward expansion and intensification of East Asian jet induced by
230 anthropogenic influence may be the reason for the weakening of the EAWM. A
231 decrease trend is found both in observation and in the All-Hist runs, therefore more
232 attention should be given to the EAWM variability under anthropogenic influence.

233

234 **Author contributions.** Xin Hao conceived the idea for the study and wrote the paper.

235 All authors contributed to the development of the method and to the data analysis.



236 **Acknowledgements**

237 This work was supported by the National Science Foundation of China (Grant
238 41421004, 41875118, 41605059 and 41505073). All datasets can be accessed publicly.
239 The NCEP analysis dataset can be downloaded from
240 <https://www.esrl.noaa.gov/psd/data>, and the simulations can be downloaded from
241 <http://portal.neresc.gov/c20c/data.html>.

242

243

244 References:

245 Boyle, J. S., and Chen, T. J.: Synoptic aspects of the wintertime East Asian monsoon,
246 in: Monsoon Meteorology, edited by: Chang, C. P. and Krishnamurti, T. N.,
247 Oxford University Press, 125–160, 1987.

248 Cui, X. P., and Sun, Z. B.: East Asian winter monsoon index and its variation analysis.
249 J. Nanjing Inst. Meteo., 22, 321–325, 1999. (in Chinese)

250 Chang, C. P., Wang, Z., and Hendong, H.: The Asian winter monsoon, in: The Asian
251 Monsoon, edited by Wang, B., Springer Press, 89–127, 2006.

252 Christidis, N., Stott, P. A., Scaife, A. A., Arribas, A., Jones, G. S., Copsey, D., Knight,
253 J. R., and Tennant, W.J.: A new HadGEM3-A-based system for attribution of
254 weather- and climate-related extreme events, *J. Climate*, 26, 2756–2783.
255 doi: 10.1175/JCLI-D-12-00169.1, 2013.

256 Collins, M., Knutti, R., Arblaster, J., Dufresne, J. L., Fichefet, T., Friedlingstein, P.,
257 Gao, X., Gutowski, W. J., Johns, T., Krinner, G., Shongwe, M., Tebaldi, C.,
258 Weaver, A. J., and Wehner, M.: Long-term climate change: projections,
259 commitments and irreversibility, In: Climate Change 2013: The Physical Science
260 Basis, Contribution of Working Group I to the Fifth Assessment Report of the
261 Intergovernmental Panel on Climate Change, edited by Stocker, T. F., Qin, D.,
262 Plattner, G. K., Tignor, M., Allen, S. K., Boschung, J., Nauels, A., Xia, Y., Bex,
263 V., and Midgley, P. M., Cambridge University Press, Cambridge, UK and New
264 York, NY, 2013.

265 Gan, B. L., Wu, L. X., Jia, F., Li, S. J., Cai, W. J., Nakamura, H., Alexander, M. A.,



- 266 and Milley, A. J.: On the response of the Aleutian Low to Greenhouse Warming,
267 J. Climate, 30, 3907–3925, 2017.
- 268 Gong, D. Y., Wang, S. W., and Zhu, J. H.: East Asian winter monsoon and Arctic
269 Oscillation. Geophys. Res. Lett., 28, 2073–2076, 2001.
- 270 Guo, Q. Y.: Relationship between the variations of East Asian winter monsoon and
271 temperature anomalies in China. Q. J. Appl. Meteorol., 5, 218–225, 1994. (in
272 Chinese)
- 273 Hao, X., Li, F., Sun, J. Q., Wang, H. J., and He, S. P.: Assessment of the response of
274 the East Asian winter monsoon to ENSO-like SSTAs in three U.S. CLIVAR
275 Project models. Inter. J. Climatol., 36, 847–866, 2016.
- 276 Hao, X., and He, S. P.: Combined effect of ENSO-like and Atlantic Multidecadal
277 Oscillation on the interannual variability of the East Asian winter monsoon. J.
278 Climate, 30, 2697–2716, 2017.
- 279 He, S. P., Wang, H. J., and Liu, J.: Changes in the relationship between ENSO and
280 Asia-Pacific midlatitude winter atmospheric circulation, J. Climate, 26, 3377–
281 3393, 2013.
- 282 He, S. P., and Wang, H. J.: Oscillating relationship between the East Asian winter
283 monsoon and ENSO, J. Climate, 26, 9819–9838, 2013.
- 284 Hong, J. Y., Ahn, J. B., and Jhun, J. G.: Winter climate changes over East Asian region
285 under RCP scenarios using East Asian winter monsoon indices, Clim. Dyn., 48,
286 577–595, doi:10.1007/s00382-016-3096-5, 2017.
- 287 Hu, Z. Z., Bengtsson, L., and Arpe, K.: Impact of global warming on the Asian winter
288 monsoon in a coupled GCM. J. Geophys. Res., 105, 4607–4624.
289 doi:10.1029/1999JD901031, 2000.
- 290 Hu, Y., and Fu, Q.: Observed poleward expansion of the Hadley circulation since
291 1979. Atmos. Chem. Phys., 7, 5229–5236, 2007.
- 292 Hu, Y., Tung, K. K., and Liu, J.: A closer comparison of early and late winter
293 atmospheric trends in the Northern-Hemisphere, J. Climate, 18, 2924–2936,
294 2005.
- 295 Hori, M. E., and Ueda, H.: Impact of global warming on the East Asian winter



- 296 monsoon as revealed by nine coupled atmosphere ocean GCMs. *Geophys. Res.*
297 *Letts.*, 33, L03713. doi:10.1029/2005GL024961, 2006.
- 298 Intergovernmental Panel on Climate Change (IPCC): *Climate Change 2013: The*
299 *Physical Science Basis, Contribution of Working Group I to the Fifth Assessment*
300 *Report of the Intergovernmental Panel on Climate Change*, Stocker, T. F., Qin, D.,
301 Plattner, G. K., Tignor, M., Allen, S. K., Boschung, J., Nauels, A., Xia, Y., Bex,
302 V., and Midgley, P. M., Cambridge University Press, Cambridge, UK, 2013.
- 303 Jhun, J. G., and Lee, E. J.: A new East Asian winter monsoon index and associated
304 characteristics of the winter monsoon. *J. Climate*, 17, 711–726, 2004.
- 305 Jiang, Y., Yang, X. Q., Liu, X., Yang, D., Sun, X., Wang, M., Ding, A., Wang, T., and
306 Fu, C.: Anthropogenic aerosol effects on East Asian winter monsoon: The role of
307 black carbon-induced Tibetan Plateau warming, *J. Geophys. Res. Atmos.* 122,
308 doi:10.1002/2016JD026237, 2017.
- 309 Kalnay, E., Kanamitsu, M., Kistler, R., Collins, W., Deaven, D., Gandin, L., Iredell,
310 M., Saha, S., White, G., Woollen, J., Zhu, Y., Chelliah, M., Ebisuzaki, W.,
311 Higgins, W., Janowiak, J., Mo, K. C., Ropelewski, C., Wang, J., Leetmaa, A.,
312 Reynolds, R., Jenne, R., and Joseph, D.: The NCEP/NCAR 40-year reanalysis
313 project, *Bull. Amer. Meteorol. Soc.*, 77, 437–470, 1996.
- 314 Kimoto, M.: Simulated change of the east Asian circulation under global warming
315 scenario, *Geophys. Res. Letts.*, 32, L16701, doi:10.1029/2005GL023383, 2005.
- 316 Lau, K. M., and Li, M. T.: The monsoon of East Asia and its global associations-A
317 survey, *Bull. Amer. Meteorol. Soc.*, 65, 114–125, 1984.
- 318 Lee, S. S., Kim, S. H., Jhun, J. G., Ha, K. J., and Seo, Y. W.: Robust warming over
319 East Asia during the boreal winter monsoon and its possible causes, *Environ. Res.*
320 *Letts.*, 8:034001(6pp), 2013.
- 321 Li, F., Wang, H. J., and Gao, Y. Q.: Change in sea ice cover is responsible for
322 non-uniform variation in winter temperature over East Asia, *Atmos. Ocean. Sci.*
323 *Letts.*, 8, 376–382, 2015.
- 324 Li, F., and Wang, H. J.: Relationship between Bering sea ice cover and East Asian
325 winter monsoon year-to-year variations, *Adv. Atmos. Sci.*, 30, 48–56, 2013.



- 326 Li, Q., Zhang, R. H., and Wang, Y.: Interannual variation of the wintertime fog-haze
327 days across central and eastern China and its relation with East Asian winter
328 monsoon, *Int. J. Climatol.*, 36, 346–354, 2016.
- 329 Li, S., He, S. P., Li, F., and Wang, H. J.: Simulated and projected relationship between
330 the East Asian winter monsoon and winter Arctic Oscillation in CMIP5 models,
331 *Atmos. Ocean. Sci. Lett.*, 11, 417–424, 2018.
- 332 Meehl, G. A., Stocker, T. F., Collins, W. D., Friedlingstein, P., Gaye, A. T., Gregory, J.
333 M., Kitoh, A., Knutti, R., Murphy, J. M., Noda, A., Raper, S. C. B., Watterson, I.
334 G., Weaver, A. J., and Zhao, Z. C.: Global climate projections, In: *Climate
335 Change 2007: The Physical Science Basis, Contribution of Working Group I to
336 the Fourth Assessment Report of the Intergovernmental Panel on Climate
337 Change*, edited by Solomon, S., Qin, D., Manning, M., Chen, Z., Marquis, M.,
338 Averyt, K. B., Tignor, M., and Miller, H. L., Cambridge University Press,
339 Cambridge, UK and New York, NY, 2007.
- 340 Mitas, C. M., and Clement, A.: Has the Hadley cell been strengthening in recent
341 decades? *Geophys. Res. Lett.*, 32, L03809, doi:10.1029/2004GL021765, 2005.
- 342 Sun, B. M., and Li, C. Y.: Relationship between the disturbances of East Asian trough
343 and tropical convective activities in boreal winter. *Chinese Sci. Bull.*, 42, 500–
344 504, 1997. (in Chinese)
- 345 Wang, B., Wu, Z. W., Chang, C. P., Liu, J., LI, J. P., and Zhou, T. J.: Another Look at
346 interannual-to-interdecadal variations of the East Asian winter monsoon: the
347 northern and southern temperature modes, *J. Climate*, 23, 1495–1512, 2010.
- 348 Wang, H. J., and Jiang, D. B.: A new East Asian winter monsoon intensity index and
349 atmospheric circulation comparison between strong and weak composite.
350 *Quaternary Sci.*, 24, 19–27, 2004. (in Chinese)
- 351 Wang, L., Huang, R. H., Gu, L., Chen, W., and Kang, L. H.: Interdecadal Variations of
352 the East Asian winter monsoon and their association with quasi-stationary
353 planetary wave activity, *J. Climate*, 22, 4860–4872, 2009.
- 354 Xu, M. M., Xu, H. M., and Ma, J.: Responses of the East Asian winter monsoon to
355 global warming in CMIP5 models, *Int. J. Climatol.*, 36, 2139–2155,



356 doi:10.1002/joc.4480, 2016.

357 Zhang, Y., Sperber, K. R., Boyle, J. S., Dix, M., Ferranti, L., Kitoh, A., Lau, K. M.,
358 Miyakoda, K., Randall, D., Takacs, L., and Wetherald, R.: East Asian winter
359 monsoon: Results from eight AMIP models, *Clim. Dyn.*, 13, 797–820, 1997.

360 Zhou, W., Chan, C. L. J., Chen, W., Ling, J., Pinto, J. G., and Shao, Y. P.:
361 Synoptic-scale controls of persistent low temperature and icy weather over
362 southern China in January 2008, *Mon. Weather Rev.*, 137, 3978–3991, 2009.

363

364

365 Figure caption:

366

367 Figure 1 Climatology of winter-mean (DJF) (a) surface air temperature (shading, °C)
368 (c) 500 hPa geopotential height (shading, m) during 1960–2012, based on NCEP
369 reanalysis data. (b), (d) As in (a), (b), but for the model’s All-Hist runs. (e)
370 Taylor diagram of winter-mean climatology for surface air temperature (TAS;
371 25 °–45 °N, 105 °–145 °E) and 500 hPa geopotential height (H500; 25 °–45 °N,
372 105 °–145 °E). The rectangle marks the areas used to calculate the climatology in
373 taylor diagram.

374

375 Figure 2 (a) The time series of the normalized EAWMI_SAT (curve) and their linear
376 trend (line) during 1960–2012, based on NCEP reanalysis dataset (top), outputs
377 of model in All-Hist run (middle), and outputs of models in Nat-Hist run
378 (bottom). (b) As in (a), but for the EAWMI_HGT. “tr” is an abbreviation for
379 “linear trend coefficient”. “*” means the tr is significant at 95% confidence level
380 based on the Mann-Kendall test, and “’ ” means the tr is significant at 90%
381 confidence level. “cor” is an abbreviation for “correlation coefficient between
382 simulated EAWM index under All-Hist scenario and observed EAWM index”,
383 “cor_dec” is an abbreviation for “correlation coefficient in decadal time-scale”.
384 Note that the time series of the EAWM indices base on outputs of model in the
385 Nat-Hist runs are standardized by the climatology simulated by the All-Hist runs.



386

387 Figure 3 Composite differences of winter-mean (a) surface air temperature
388 (shading, °C) and (b) 500 hPa geopotential height (shading, m) between the
389 All-Hist runs and Nat-Hist runs, during 1960–2012. The plus signs denotes
390 where the composite differences are significant at the 95% confidence level
391 based on two-sided Student *t* test.

392

393 Figure 4 Composite differences of winter-mean (a) air temperature (shading, °C) over
394 90°E–150°E, (b) 250 hPa zonal wind (shading, m/s) and (c) sea level pressure
395 (shading, hPa) and 850 wind (vector, m/s) between the All-Hist runs and
396 Nat-Hist runs, during 1960–2012. Red contours denote the climatology of
397 All-Hist runs. The plus signs denotes where the composite differences are
398 significant at the 95% confidence level based on two-sided Student *t* test.

399

400 Figure 5 (a) The number of strong EAWM events during 1960–2012, based on NCEP
401 reanalysis dataset (left), outputs of model in the All-Hist runs (middle), and
402 outputs of model in the Nat-Hist runs (right). (b) As in (a), but for weak EAWM
403 events.

404

405

406

407

408

409

410

411

412

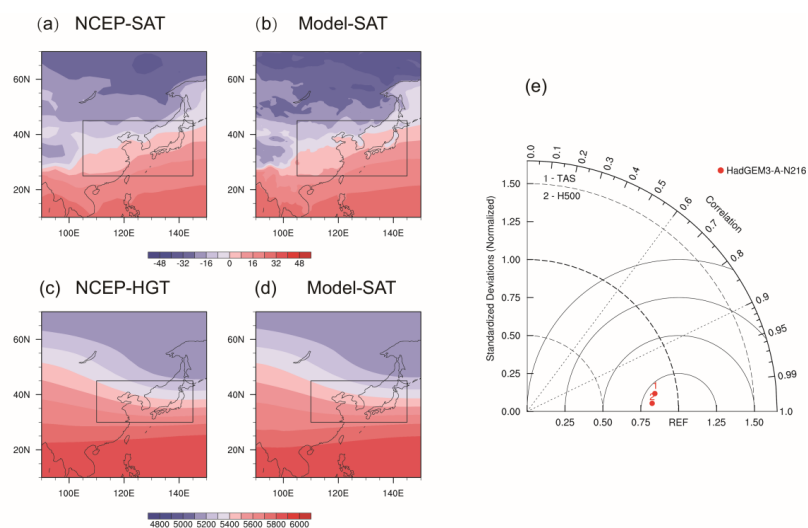
413

414

415

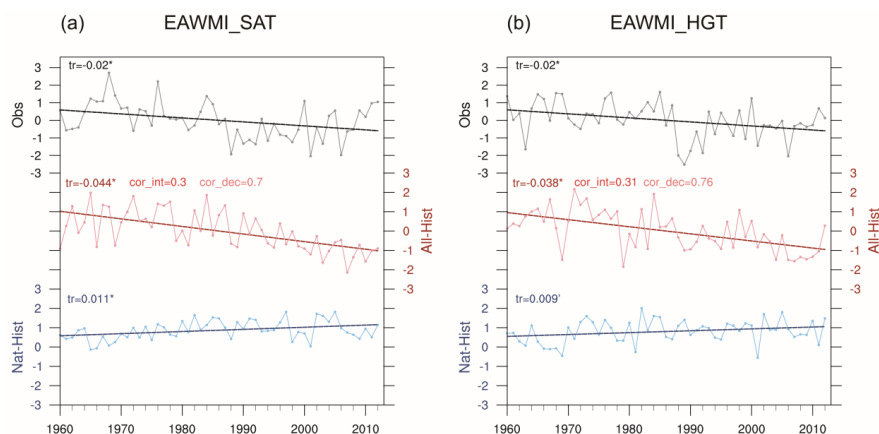


416 Figures



417

418 Figure 1 Climatology of winter-mean (DJF) (a) surface air temperature (shading, °C)
 419 (c) 500 hPa geopotential height (shading, m) during 1960–2012, based on NCEP
 420 reanalysis data. (b), (d) As in (a), (b), but for the model's All-Hist runs. (e)
 421 Taylor diagram of winter-mean climatology for surface air temperature (TAS;
 422 25°–45°N, 105°–145°E) and 500 hPa geopotential height (H500; 25°–45°N,
 423 105°–145°E). The rectangle marks the areas used to calculate the climatology in
 424 Taylor diagram.

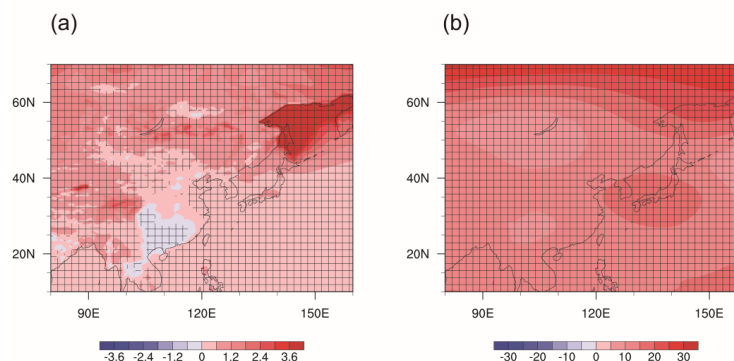


425

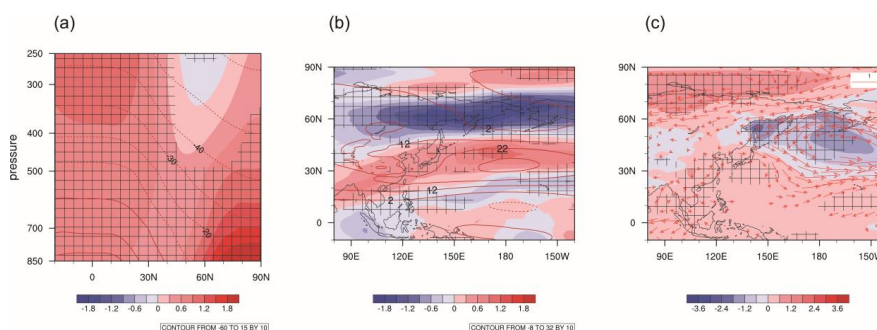
426 Figure 2 (a) The time series of the normalized EAWMI_SAT (curve) and their linear
 427 trend (line) during 1960–2012, based on NCEP reanalysis dataset (top), outputs



428 of model in All-Hist run (middle), and outputs of models in Nat-Hist run
429 (bottom). (b) As in (a), but for the EAWMI_HGT. “tr” is an abbreviation for
430 “linear trend coefficient”. “*” means the tr is significant at 95% confidence level
431 based on the Mann-Kendall test, and “’ ” means the tr is significant at 90%
432 confidence level. “cor” is an abbreviation for “correlation coefficient between
433 simulated EAWM index under All-Hist scenario and observed EAWM index”,
434 “cor_dec” is an abbreviation for “correlation coefficient in decadal time-scale”.
435 Note that the time series of the EAWM indices base on outputs of model in the
436 Nat-Hist runs are standardized by the climatology simulated by the All-Hist runs.



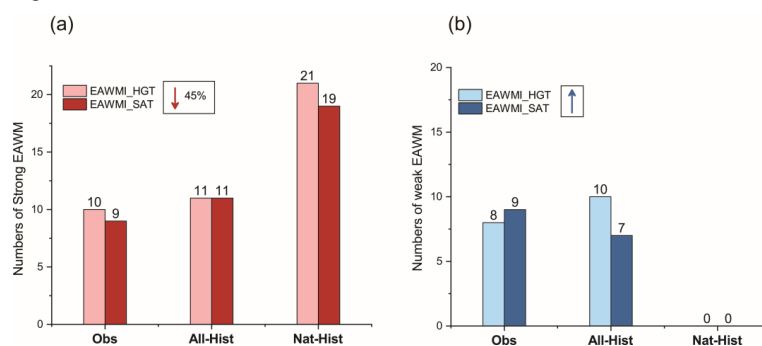
437
438 Figure 3 Composite differences of winter-mean (a) surface air temperature
439 (shading, °C) and (b) 500 hPa geopotential height (shading, m) between the
440 All-Hist runs and Nat-Hist runs, during 1960–2012. The plus signs denotes
441 where the composite differences are significant at the 95% confidence level
442 based on two-sided Student *t* test.



443
444 Figure 4 Composite differences of winter-mean (a) air temperature (shading, °C) over



445 90 °E–150 °E, (b) 250 hPa zonal wind (shading, m/s) and (c) sea level pressure
446 (shading, hPa) and 850 wind (vector, m/s) between the All-Hist runs and
447 Nat-Hist runs, during 1960–2012. Red contours denote the climatology of
448 All-Hist runs. The plus signs denotes where the composite differences are
449 significant at the 95% confidence level based on two-sided Student *t* test.



450
451 Figure 5 (a) The number of strong EAWM events during 1960–2012, based on NCEP
452 reanalysis dataset (left), outputs of model in the All-Hist runs (middle), and
453 outputs of model in the Nat-Hist runs (right). (b) As in (a), but for weak EAWM
454 events.

455
456
457